7-2015

Characterization of Human Muscle Extracellular Matrix

Lauren Klaire Wilson
University of Arkansas, Fayetteville

Characterization of Human Muscle Extracellular Matrix

Characterization of Human Muscle Extracellular Matrix

A thesis submitted in partial fulfillment
of the requirements for the degree of
Master of Science in Biomedical Engineering

by

Lauren Wilson
University of Arkansas
Bachelor of Science in Biological Engineering, 2013

July 2015
University of Arkansas

This thesis is approved for recommendation to the Graduate Council.

_____
Dr. Jeff Wolchok
Thesis Director

_____
Dr. Narasimhan Rajaram
Committee Member

_____
Dr. Tyrone Washington
Committee Member

Abstract

The performance of extracellular matrix (ECM) biological scaffolds for the treatment of volumetric muscle loss (VML) has shown promising results with regenerating native muscle in animal models and human patients. However, the limitations of these scaffolds include non-specific characteristics based on the original parameters of the muscle that is lost and this is why our group chose to characterize human skeletal ECM. By understanding the characteristics of the native human skeletal ECM, more desired queues for the biological scaffolds being used to treat VML can be provided. Upper limb and lower limb skeletal muscles were commercially obtained, decellularized using common techniques, and underwent biochemical and physical assessment. The presence of collagen and glycosaminoglycans were identified within the human skeletal ECM. The mechanical strength and overall alignment of the human skeletal ECM was also evaluated. The human skeletal ECM supported an in-vivo degradation assessment and showed signs of tolerance within the in-vivo model. The results of the current study suggest that the location and gender of the original muscle indeed plays a significant role between the two ECM muscle types within some of the characterization tests. We believe we are the first group to characterize human skeletal muscle ECM with the intent to mimic these parameters. A future direction for this project would be to incorporate these parameters found within this study into our engineered ECM being produced within our lab.

Acknowledgments

Special thanks is due to my advisor for taking letting me gain laboratory experience as an undergraduate and taking me on as a masters student. A special thanks is given to my undergraduate colleague, Abby Terlouw for running one of my characterization assays and John Kim, a PhD graduate student in our lab, for proofreading my thesis.

Table of Contents

1. Introduction

1.1 Muscle and Acute Muscle Injuries/Self Repair

Muscle is a fibrous tissue that contributes to different voluntary and involuntary movements throughout the body. Muscle can be grouped in three different categories: skeletal muscle, smooth muscle, and cardiac muscle. The focus of this study is within the scope of skeletal muscle, which is termed a voluntary muscle that is anchored to the bones by tendons and ligaments. More specifically skeletal muscle is composed of myofibers and connective tissue[1]. Myofibers, capillaries, and nerves are housed within the connective tissue. Its main function to skeletal muscle is providing a framework so muscles can contract. The myofibers are the components that are interacting with the nerves in order to carry out contraction forces for skeletal muscle. The basic structure that groups myofibers into myofibrils is a connective tissue structure composed of three different layers or sheets[2]. The epimysium layer is considered to be the outer most layer that holds all of the myofibrils together since it surrounds entire muscle. The epimysium layer is the strongest layer within the connective tissue structure that house the myofibrils. The epimysium layer is made of multiple fascicles that house the myofibrils. The outer layer of the fascicles is the second/middle layer of the connective structure called the perimysium. Within the fascicles is the home of the third inner-most layer of the connective tissue structure called the endomysium. The endomysium is a dense sheath that surrounds each individual myofiber within the myofibril bundle. The extracellular space outside of each individual myofiber and the bundles of myofibrils houses the extracellular matrix. The

extracellular matrix (ECM) is composed of multiple cellular and structural components that help with muscle repair/regeneration following acute muscle injury.

Acute muscle injury can occur from multiple sources. For example, strain related muscles injuries[3], lacerations[4], and contusions[5] are all injuries that can be repaired by existing muscle surrounding the site of injury. The process of muscle self-repair following one of these acute injuries follows three main steps. This is a brief review of the main points in muscle self-repair/regeneration. Muscle self-repair involves more signals than the ones described in this study. The first stage in muscle-repair is inflammation at the site of injury[6]. Leukocytes, mainly neutrophils and macrophages are recruited to the site of the injured muscle and start to remove necrotic muscle tissue at the injury site by phagocytosis. Evidence suggests macrophages have another function within muscle regeneration[6]. Cultured activated macrophages along with skeletal muscle myoblasts from neonatal rats have been shown to increase myoblast number size and proliferation. An increase of myotubes were also found within cell cultures containing the activated macrophages and myoblasts. This suggests that once an inflammatory response is over at the site of injury, macrophages continue to play a role in muscle self-repair. Once the initial inflammatory response is over, satellite cells already located between the plasma membrane of myofibrils and the endomysium layer become activated at the site of injury[7]. Satellite cells are the "stem cells" for muscle; they are responsible for repair and regeneration of skeletal muscle. Activation of satellite cells can be complex. One way these cells are activated is by nitric oxide (NO) synthesis. The macrophages that are recruited to the injured muscle site produce NO as a side product of phagocytosis of the necrotic muscle tissue. The NO is then synthesized and this stimulates the release of hepatocyte growth factor (HGF) that is stored within the ECM of skeletal muscle. Once the HGF is released it can bind to c-met receptors on the surface of the

satellite cells in the muscle, thus activating satellite cells in response to injury[8,9]. After satellite cells are activated, they must proliferate and differentiate into muscle cells. Proliferation and differentiation of the satellite cells into multinucleated myofibers and then into myofibrils is achieved through two different signaling pathways. Notch-1 pathways are believed to become activated within a satellite cell at the first site of injury and then this pathway immediately starts satellite cell proliferation[10]. Eventually the Notch-1 pathway transitions into the Wnt pathway for differentiation of satellite cells[11]. The satellite cells differentiate into myofibers and then the myofibers get bundled together to make myofibrils.

1.2 Severe muscle loss and current treatments

Muscle that has been severely damaged does not undergo self-repair/regeneration. This type of muscle damage is termed volumetric muscle loss (VML) and scar tissue replaces the once healthy tissue causing major functional loss at the site of injury. Volumetric muscle loss is defined as skeletal muscle that is lost due to trauma that exceeds the muscle's ability to repair the affected site[12]. VML mostly occurs from extensive military injuries[13], but can also occur from extreme sporting accidents, gunshot wounds or birth defects. Treatment is required in order to try and improve functional mobility at the site of injury. Current treatment methods for VML include removal of scar tissue and the implantation of muscle flaps[14]. Scar tissue is initially removed to help improve the chance of regaining some form of functionality back into the VML site. Muscle flap transfers are usually autologous and are taken from the back muscles, since these muscles offer a large surface area. The muscle flaps are surgically placed over the VML site, however the flaps are generally just used as a covering to prevent infection and protect

exposed muscle and bone. Patients who undergo muscle flap surgery to treat a VML wound site can regain some basic function at the injured site, but usually never regain full function of the lost muscle[14]. Therefore, different experimental methods are being investigated for treatment of volumetric muscle.

1.3 New techniques in treating VML

The main goal when studying these new techniques is to ultimately give the patient full function at the VML site and restore native muscle formation. There are two different approaches to treating VML that are being studied in current literature. One is using extracellular matrix (ECM) derived from existing muscle to help regenerate native muscle within the VML site in animal models and extreme human cases [15-18], and the other technique, which is currently being investigated in our lab, is using "engineered" ECM[19] derived from skeletal muscle cells to regenerate native skeletal muscle in a rat animal model.

Native ECM is being derived from multiple locations within the body and is being used as a treatment method for VML. In one study, rat tibilias anterior (TA) was decellularized and its corresponding skeletal ECM was implanted into a VML defect[15]. The VML criteria for this particular study involved removing 20% of the original muscle mass from the TA of their rat animal model. The implantation site was observed at 2, 4, and 6 months post-surgery. This group did find some evidence of muscle regeneration within the defect site around the 2 and 4 month time points. Treatment of VML with decellularized ECM derived components has also been studied within a human trial where the patient suffered from a massive skeletal muscle

(quadriceps) injury[16]. The patient's quadriceps injury was treated with a manufactured implant that consisted of porcine small intestinal submucosa (SIS) ECM. This material (Restore) was commercially obtained from DePuy Orthopaedics, Inc in Warsaw, Indiana. New tissue growth was reported after 36 weeks post-surgery, and the patient regained some function at the injury site as time progressed. Another VML model treated with decellularized porcine small intestinal submucosa ECM was tested within mice, and results observed were similar to those described in the previous studies listed above[17]. A new human trial study that performed VML treatment on 5 patients using a porcine urinary bladder derived ECM has recently been published[18]. These 5 patients all had lower limb skeletal muscle VML injury sites. The importance of this study was that 3 of the 5 patient's involved experienced functional improvement at the injury site six months after the original surgery. All of these results however are still not enough evidence to completely eliminate the muscle flap option as the current treatment method for VML.

The second approach to treating VML with the hopes of regenerating new native skeletal muscle is engineering ECM (eECM) from skeletal muscle cells[19]. This technique of engineering an extracellular matrix is still fairly new. An in vivo study was performed within a rat animal model to observe the degradation time and inflammation response generated from the eECM. A VML site was not generated in this model but the eECM implant was placed within a surgically induced pouch within this model. By the first time point at 4th weeks after implantation, the eECM was still degrading and evidence suggested remodeling at the implant site. By the 12th week after implantation of the eECM, the implant was completely degraded and no evidence of chronic inflammation was observed. This suggests the eECM derived from skeletal muscle cells could be a possible treatment for VML. Based on these characteristics found from the eECM

produced within our lab, more desirable traits based on human skeletal muscle ECM was investigated to enhance existing eECM traits.

1.4 Objectives

The main objective of the present study was to characterize human skeletal muscle extracellular matrix (ECM). More specifically, characterize and understand the properties of human rectus femoris ECM and human supraspinatus ECM. Lastly, compare the two different human skeletal ECM locations along with comparing female ECM to male ECM.

1.5 Key Chemical ECM characteristics: (Components)

Extracellular matrix (ECM) is a group of cellular components that surround different tissues and organs to perform specific functions. ECM structure and composition is different based on the location of the tissue/organ it surrounds. Generally, ECM consists of collagen, glycosaminoglycans, proteoglycans, and glycoproteins. ECM has multiple functions that include: cell adhesion, cell proliferation, cell differentiation, cell structural support, and tissue regeneration. These functions are carried out by the different cellular components within the ECM.

Collagen is the most abundant protein within the ECM. Different types of collagen have been identified and characterized within different types of ECM, however collagen I is the most common in most ECM. ECM that contains collagen I usually possess different collagen types,

but in smaller amounts. For example, type I, II, III[20,21], IV, V-VIII[22], and XI-XIII[22] have all been identified within skeletal muscle ECM. Collagen is important for its structural and mechanical function due in part to the alignment of the proteins and the recruitment of cells to the ECM[23]. Collagen fibers form into many different types of collagen fibrils. Collagen has a triple helix that is composed of three helical polypeptides. The presence of collagen within materials is usually identified through the presence of hydroxy-proline. Hydroxy-proline is one of the amino acids that makes up the polypeptides alpha helices. Hydroxy-proline makes up 13.5%[24] of collagen, making it a predominant identifier when looking for the presence of collagen. Homologous regions within the triple helix of individual collagen types are responsible for the formation of fibrils; therefore collagen is one of the main components that provides structural support to ECM[25]. Certain collagen types have been shown to help with cell attachment. Collagen type I has been proven to enhance cell attachment, proving collagen type I promotes cells to adhere to the ECM[26]. When exposed to different cell types, collagen types I and II have been shown to induce differentiation of certain cell populations, maturation of cell populations, and maintain overall survival of cell populations[27]. The results of different interactions with collagen types I and II indicate ECM has the potential to stimulate differentiation, proliferation, and survival of multiple cell types.

Glycosaminoglycans (GAG) and proteoglycans (PG) components serve cellular and structural functions within the ECM. Proteoglycans are proteins that consist of a “core protein” with one or more covalent glycosaminoglycan side chains[28]. Glycosaminoglycans are very large and do not fold. This results in the ECM having a large surface area around the corresponding tissues. In general, proteoglycans are negatively charged causing an osmotic imbalance resulting in water entering the ECM. This results in hydrating the ECM as well as providing support

against compressive forces acting upon the ECM. GAGs and proteoglycans also serve cellular functions within the ECM. The most common GAG side chains, chondroitin sulfate, dermatan sulfate, and heparan sulfate have all been identified within skeletal muscle ECM[29,30]. Decorin, a proteoglycan with either a chondroitin sulfate or dermatan sulfate GAG side chain, has been studied extensively[21,31]. Decorin has been proven to bind to collagen types I-IV within ECM indicating its role in helping the initiation of fibril formation of collagen fibers. Other dermatan sulfate and heparan sulfate proteoglycans have been shown to bind to fibronectin, another ECM component[32,33]. These interactions show how different cellular components of ECM interact with each other. Another class of proteoglycans, chondroitin sulfate, with a chondroitin sulfate GAG side chain, has been studied in regenerating skeletal muscle[34]. Chondroitin sulfate has been proven to be synthesized within regenerating skeletal muscle; however chondroitin sulfate has not been proven to inhibit or enhance the production of regenerating skeletal muscle. More studies on this particular PG with a chondroitin sulfate GAG side chain should be performed in order to conclude its role in the ECM.

Cellular fibronectin and laminin are glycoproteins within ECM[35]. Fibronectin and laminin have been studied extensively on how they interact with cells when exposed to different conditions. Both fibronectin and laminin promote cell adhesion, indicating they can attract cells to attach to ECM[26]. Fibronectin[36,37] and laminin[37] have been shown to enhance cellular attachment of collagen type I and IV with other cell types in vitro. Both glycoproteins also promote proliferation of cells[38]. This function of fibronectin and laminin indicates when cells attach to ECM, they have the ability to proliferate.

1.6 Key Physical ECM characteristics: (Mechanics and Architecture)

ECM has specific mechanical and architectural properties based on the original location of the muscle it originated from[39]. Since ECM properties mimic the properties of the original muscle, skeletal muscle ECM has a more distinct architecture than other ECM materials. The collagen fibers within skeletal muscle ECM are densely packed together to give the material its mechanical properties. The more aligned the collagen fibers, the stiffer the ECM material. The mechanical and architectural properties of ECM helps with the cellular functions ECM also possess[40]. Porosity is another architectural property skeletal ECM possesses. The pores are used as a pathway for cells to enter and leave the ECM. Different cells also use the pores to proliferate and differentiate while in the ECM. Usually ECM material with high mechanical properties and a distinguished architecture are used as biologic scaffolds when these parameters are needed. Some ECM materials do not require specific alignment or mechanical properties. For example, the use of cardiac derived ECM is being used as an injectable gel to help promote cardiac muscle regeneration[41]. The ECM material being used in this case does not require mechanical or architectural characteristics. The function of the ECM should be taken into consideration when deciding which properties the ECM needs to possess.

1.7 Decellularization

Since ECM has many desirable qualities for regenerating muscle/self-repair, ways of obtaining native ECM has been studied intensively. The main method to obtain native ECM is

through decellularization of tissues/organs. Decellularization is the removal of cellular components from any desired tissue/organ, and decellularization of tissue/organs can be completed using different techniques. The two most common techniques used for decellularization is a perfusion method or a constant agitation method. The main difference between the perfusion method and the constant agitation method is the mechanism each method uses to decellularize materials[42]. Perfusion decellularization uses a convective mechanism while agitation decellularization uses a diffusion-based mechanism. Convective flow is described as a moving liquid over a solid surface as a result of a pressure differential. The decellularization agent is the "moving liquid" and the material is the "solid surface" in this scenario. Diffusion works differently than convection by moving particles from a high concentration to a low concentration as a result of a concentration gradient.

The perfusion decellularization method has been performed on different types of whole organs with extensive vasculature: ferret liver, pig kidney, pig pancreas, pig intestines[43], rat hearts[44], and rat lung[45]. Perfusion decellularization involves pumping a detergent through the vasculature of the organ continuously until the material is completely decellularized. A specific example of perfusion decellularization is with the rat heart. Typically, the perfusion of the decellularization agent starts in the ascending aorta allowing the agent to continuously flow through all of the corresponding arteries and veins to eventually flow out of the left ventricle[44]. A tissue/organ is considered to be "completely decellularized" when DNA/RNA and intracellular structural proteins are removed[44]. Visual changes will occur when a tissue/organ has been decellularized. The material will gradually turn from a deep red color to a pure yellowish/ white color indicating blood and cellular components (nuclei and cellular actin) are perfusing out and eventually the components are all removed. This method produces decellularized ECM with its

original architecture, and the decellularization time is greatly reduced when compared to the agitation method.

The alternative method for decellularization is constant agitation or constant "stirring". This method is performed within a semi-large container that includes a detergent and the desired material. The container can either be placed on a rocker plate with slight agitation, or the container can be placed on a stir plate and the container would have a stir bar to provide constant agitation. Decellularization using the constant agitation/stirring method has been used in many tissues and organs: human adipose tissue from human lipoaspirate[46], porcine skeletal and cardiac tissue from intercostal muscles[22], canine quadriceps and hamstrings[47], porcine dermis and urinary bladder[48], porcine brain and spinal cord[49], and porcine myocardial ventricular tissue[50]. This method also decellularizes material well, however this method requires more time than the perfusion method. The amount of time agitation decellularization takes is dependent on the thickness and density of the tissue that's being decellularized. Depending on how much agitation is applied to the material during decellularization will determine how much of the original architecture is left intact. Both systems require a detergent, but any detergent can be used for both systems.

Two common detergents used for decellularization are Triton X-100 and sodium dodecyl sulfate (SDS). Both detergents have been compared to each other in previous studies to see which detergent is the most effective at decellularizing material. Triton X-100 is a non-ionic detergent that causes very mild effects on tissues when it is used for decellularization[51]. Non-ionic detergents use lipid-lipid interactions or lipid-protein interactions to remove cellular components from tissue/organs. Non-ionic detergents do not disrupt protein-protein interactions within tissue/organs, this insures the ECM will have the same architecture as the original

material. SDS is an ionic detergent that is also commonly used for different decellularization processes[51]. Ionic detergents disrupt protein-protein interactions when they are used for decellularization, which can disrupt the original architecture of the tissue/organ. Triton X-100 has been shown to partially remove cellular components within tissue/organs when compared to SDS[44]. SDS and Triton X-100 were both used to decellularize rat hearts, and the resulting ECM was analyzed to compare the effects both detergents had on the material[44]. Individual hearts were either decellularized with Triton X-100 or SDS using the perfusion method for 12 consecutive hours. After the allotted time, the SDS perfused heart was completely decellularized when compared to the Triton X-100 perfused heart. Visual observation of the hearts showed the SDS perfused heart was completely clear/white, while the Triton X-100 perfused heart was still pinkish/clear. These observations indicate complete removal of cells from the SDS perfused heart compared to the Triton X-100 perfused heart. Also, immunohistochemical analysis was performed on the two separate hearts. These results indicated the SDS perfused heart contained no nuclei or contractile elements. However, the Triton X-100 perfused hearts did contain small amounts of nuclei and contractile elements. This comparison proves SDS is more efficient than Triton X-100 for decellularization methods. Triton X-100 has also been compared to SDS to evaluate which detergent removes native collagen and GAG components within decellularized porcine anterior cruciate ligament[52]. The agitation decellularization method was used to compare the detergents. Both Triton X-100 and SDS removed native collagen and GAG components within the ligament equally. These observations indicate both detergents are capable of removing important ECM components from native tissue/organs.

In addition to detergents, decellularization methods can also include buffers, DNAse/RNAse inhibitor solutions, and chelating agents. The addition of EDTA with Tris-HCL

into a detergent solution enhances the decellularization process. EDTA is a chelating agent[51] that can cause cell lysis by binding to divalent cations that are present on cell adhesions to the ECM. Tris-HCL buffer is used to keep the solution containing the EDTA and detergent at an optimal pH as well as permeabilizing the outer membrane of the tissue/organ by interacting with lipopolysaccharides that are present on the membrane. EDTA paired with Tris-HCL is not known to remove cellular components from the tissue/organ, it simply opens the membrane in order for the detergent to remove the components. A DNAse/RNAse buffer along with a DNAse I and a RNAse-A solution is used on the decellularized tissue/organ to completely remove any remaining DNA/RNA the detergent could have left behind during the decellularization process. A host could experience an immune response if there is any remaining DNA/RNA within the material that is implanted. A typical DNAse/RNAse buffer consists of Tris-HCL, $MgCl_2$, NaCl, and $CaCl_2$[53]. The Tris-HCL keeps the buffer solution at the correct pH for DNA extraction (pH = 7.4), as well as permeabilizes the membrane of the tissue/organ. $CaCl_2$ acts as an activator of DNAse I, and $MgCl_2$ enhances the effect of DNAse I on DNA. The activity of DNAse I is optimized in the presence of both $MgCl_2$ and $CaCl_2$[53]. DNAse I cleaves each strand of DNA independently in the presence of $MgCl_2$, and the site of cleavage is random. Unlike DNA I, RNAse-A does not require any cofactors for its activity, but RNAse-A does require NaCl to activate it. RNAse-A removes RNA that is not specifically bound within the tissue/organ. The addition of these agents helps remove any leftover cellular debris that may be left at the end of the decellularization process.

By understanding the general functions of regular skeletal muscle and how it becomes traumatically injured as well as the current treatment methods for these injuries, the limiting factors these current treatments possess are elucidated. By characterizing human skeletal

extracellular matrix and understanding these characteristics, exploration of worthwhile alternatives to help improve current methods in volumetric muscle loss is possible.

2. Materials and Methods

2.1 Overview of experimental design

Whole human rectus femoris (RF) and supraspinatus (SS) skeletal muscle samples (n = 8/muscle type, 4 male and 4 female) were procured from a commercial tissue donation center (Science Care, Phoenix, AZ). Skeletal muscle samples were decellularized using a Tris-HCL, SDS solution and the resulting ECM biomaterial was thoroughly characterized to determine several key physical and chemical properties. Characterization tests included:

1. ECM yield (g ECM / g whole muscle)
2. Collagen content (% dry weight),
3. Glycosaminoglycan (GAG) content (% wet weight)
4. Modulus of elasticity (kPa)
5. Porosity (%)
6. Network Alignment (degrees)
7. Degradation rate (% volume loss / week)

Whole and decellularized skeletal muscle sample architecture, surface appearance and composition were qualitatively characterized using a panel of imaging techniques. The influence

of muscle harvest location (upper versus lower limb) and gender (male versus female) on each of the key parameters was evaluated.

2.2 Decellularization

Upon arrival, the RF and SS muscles were stored at -80°C. In preparation for decellularization, frozen whole muscle samples were thawed, cleaned of any residual fat and tendon, weighed, imaged, sectioned into strips or plugs, and batch decellularized following a published protocol. Samples were soaked in 1% sodium dodecyl sulphate (SDS) with 1% EDTA in Tris-HCL buffer (pH 8.0) for approximately two weeks at room temperature using gentle agitation and multiple decellularization solution exchanges. To remove nuclear remnants, samples were incubated for 12 hours at 4°C in a reaction buffer containing 1 kU/ml DNAse/RNAse. Samples were rinsed in PBS, (pH 7.4) for approximately 48 hours (4°C) to remove any residual decellularization solutions. ECM yield for each muscle sample (n = 8 / muscle type, 4 male and 4 female) was calculated as the ratio of decellularized sample weight (g) to pre-decellularization whole muscle sample weight (g). Once decellularized, the hydrated samples were either immediately utilized or frozen (-80°C) until needed for testing.

2.3 Imaging

Representative whole and decellularized skeletal muscle samples were sectioned with the aid of a cryostat (CM1860, Leica Biosystems, Buffalo Grove, IL.). Samples were fixed in 4%

paraformaldehyde, sectioned to the thickness of 15um and mounted on microscopic slides. Mounted sections were permeabilized with 0.1% Triton X-100 and blocked with 4% goat serum. Slides were immune-reacted for the presence of collagen type I (Sigma-Aldrich, 500:1), chondroitin sulphate proteoglycans (Sigma-Aldrich, dilution 500:1), and cytoskeletal actin, (Invitrogen, 50:1 dilution), followed by incubation in the appropriate fluorescently labeled secondary antibodies (Alexa 488 and 594, Invitrogen, 500:1). Sections were counter stained with the nuclear dye DAPI (Invitrogen, Grand Island, NY 1:20 dilution) and then microscopically imaged. Additionally, representative whole and decellularized muscle samples were lyophilized, sputter coated with platinum, and imaged with the aid of a scanning electron microscope.

2.4 Porosity and Orientation

Decellularized RF and SS samples were incubated in 10% formalin overnight at 4°C, paraffin embedded and sectioned in either the transverse (across muscle fibers) or longitudinal (along muscle fibers) direction with the aid of a microtome (5um). Sections were mounted on microscopic slides, stained with hematoxylin and eosin (H&E), and microscopically imaged (100X). Two representative images from each sample (n = 8 / muscle type, 4 male and 4 female) were used to measure porosity (% open space), and ECM network alignment (average oriented angle) using image analysis software (ImageJ) and guided by published techniques[54,55]. Porosity and alignment were measured from transverse and longitudinally sectioned samples respectively. The direction of muscle contraction (long axis of the RF and SS muscles) was selected to correspond to an orientation angle of 0 degrees.

2.5 Biochemical Assessment

Decellularized RF and SS sample collagen content (% dry weight) was estimated from hydroxy-proline concentration. Hydroxy-proline concentration was determined from extracted samples (n = 8 / muscle type, 4 male and 4 female) using a published technique[56]. Briefly, extracted samples were digested in a 6N HCL solution (20 hrs at 115°C) and then neutralized with sodium hydroxide. Digested samples were mixed with a chloramine T solution (1:2) and incubated at room temperature for 20 minutes. A dimethyl-aminobenzaldehyde assay solution was added (1:2) and the mixture was incubated at 65°C for 25 minutes. During this time a red chromophore develops. Chromophore intensity indicates hydroxy-proline concentration. Sample absorbance was read at 570 nm using a microplate reader. RF and SS values were compared against a standard curve, and collagen concentrations were calculated. Samples were tested in triplicate.

Glycosaminoglycan concentrations of human RF and SS ECM samples (n = 8 / muscle type, 4 male and 4 female) were determined with the Blyscan Sulfated Glycosaminoglycan Assay Kit (Biocolor Ltd., Carrickfergus, Co Antrium, United Kingdom). Briefly, samples were digested using a papain extraction reagent method. Samples were digested at a concentration of 30-40 mg (wet weight) per 1.5 ml of papain reagent at 65°C for 3 hours. Digested samples and standards were treated with Blyscan dye reagent then treated with dissociation reagent. Samples and standards were run in triplicate on a ninety six-well plate and read at an absorbance of 656 nm.

2.6 Mechanical Testing

In preparation for mechanical testing, RF and SS muscle sample (n = 8/ muscle type; 4 male and 4 female) were thawed at room temperature and sectioned into 3cm X 0.5cm strips aligned in the direction of muscle contraction. Uniaxial tensile testing was accomplished with the aid of a computer controlled material testing system (Model, Instron, Norwood, MA) incorporating a 10N load cell. Manufacturer software (Bluehill® Lite, Instron, Norwood, MA) was used to control strain rate and record force/elongation data. The long axis of hydrated samples (PBS) was aligned in the direction of loading and secured at each end using hand tightened serrated grips. A gauge length of 2 cm was used for all samples. Prior to tensile testing, samples were pre-conditioned using 5 cycles of 10% strain to establish a uniform loading history for all samples. Immediately following pre-conditioning, each sample was loaded to failure at a quasi-static strain rate of 10 mm/min. Raw data were collected at a sampling rate of 10Hz. For each tissue sample, engineering stress versus strain curves were generated from load and elongation data. From these curves, the tangent modulus was calculated as the slope of a linear curve fit to the stress-strain region extending from the end of the toe-in region (5%) to 20% strain. Secant moduli, at 10% and 20% strain were also calculated.

2.7 In-vivo Degradation

In-vivo degradation was examined using a dorsal subcutaneous implant site in a mouse model. *In-vivo* degradation was assayed at short-term (4 weeks) and mid-term (8 weeks) time points (n = 4/time point). Male outbred mice (CD1, Harlan, Indianapolis IN) were used for all

time points tested. All surgical procedures were performed in accordance with protocols approved by the University of Arkansas Institutional Animal Care and Use Committee. Anesthesia was induced via IP injection of a ketamine/xylazine cocktail. The subcutaneous implant site was surgically exposed through a 2 cm left-right incision placed 2 finger widths caudal to the scapulae. A subcutaneous pouch was created in each animal by blunt dissection. A single ECM disk (approximate size 9.5mm x 3mm) prepared from decellularized RF muscle was implanted into each pouch (approximate implant size). Incisions were closed using surgical adhesive (VetBond, 3M). Following surgery all animals were housed in the University of Arkansas Central Laboratory Animal Facility. At the prescribed time-points (4 and 8 weeks) all were euthanized via inhalation of carbon dioxide. The implant site with surrounding soft tissue was harvested and imaged. From the images, implant diameter was measured and used as a metric of ECM degradation.

2.8 Statistical Analysis

All data is presented as the mean ± the standard error of the mean, except for the ages and weights of each sample, which is presented as mean ± standard deviation. The yield, collagen content, GAG content, elastic modulus, elastic modulus at 10% strain, porosity, and oriented angle were all analyzed with a two-way analysis of variance (ANOVA) and a student two tailed t-test assuming equal variance. The half – life was recorded for the degradation of the ECM pellet. Significance difference was reported as $P < 0.05$ for all data. All of the ANOVA's were performed using JMP software (JMP Statistical Discovery from SAS, Cary, NC), and all student t-tests were performed using Microsoft Excel.

3. Results

The average age of all of the samples (RF and SS) was recorded at 71.32 ± 19.59 years old, while the average age of the RF samples and the SS samples were 70.0 ± 22.14, and 65.8 ± 22.90 years old, respectively (Table 1). The ages of RF samples ranged from lowest to highest, 24 (male) – 98 (female), while the SS samples ranged 24 (male) – 95 (male). The full RF and SS muscles were visually inspected before the decellularization process began (Fig, 1, A, B). The weights of the rectus femoris and the supraspinatus varied greatly, which is to be expected since the RF is larger than the SS. There was a significant difference between the weights of the rectus femoris and supraspinatus, but no significant difference was observed for the ages of the different skeletal muscles. The weight of the RF samples averaged 79.16 ± 30.48 grams, while the SS averaged 19.16 ± 5.48 grams (Fig. 1, C).

The progress of decellularization for RF samples was visually recorded at Day 0, 5, and 15 (Fig. 2, A) with Day 0 being before decellularization. Immunohistochemistry was also performed on non-decellularized and decellularized RF samples to observe the presence of nuclei and intercellular actin. The DAPI stain revealed multiple nuclei and the presence of actin in the non-decellularized sample, which is to be expected since those samples did not undergo any treatment (Fig. 2, B). The decellularized RF ECM did not show any nuclei present, the sample did however show some evidence of background staining for the actin, but actin was not expressed in the decellularized stain (Fig. 2, C).

Images were taken of RF ECM at a low magnification with a digital camera and high magnification with a SEM microscope. The low magnification image revealed how much material was left after decellularization as well as some indication of alignment (Fig. 3, A). The SEM image revealed a magnified look at the fibers within the ECM (Fig. 3, B). The fibers are all intertwined with each other with indication of alignment.

The amount of material salvaged from both RF and SS samples after decellularization was closely related. The RF ECM samples (both male and female) has a slightly higher yield (21.44 ± 3.86%) than the SS ECM samples (both male and female), 19.10 ± 3.72% (Fig. 3, C). The female RF ECM samples (26.43 ± 6.34%) produced a slightly higher yield than the SS female ECM samples (21.22 ± 7.40%). The male RF ECM samples (16.44 ± 3.57%) and the male SS samples (16.98 ± 2.65%) produced similar amounts of ECM material.

The presence of collagen within the RF ECM after decellularization was observed after immunofluorescence staining (Fig. 4, A). The collagen content of the RF ECM and the SS ECM was significantly different from each other with 2.27 ± 0.31% and 4.78 ± 1.05% (Fig. 4, B). The male and female samples within the RF ECM were similar to each other with 2.45 ± 0.57% and 2.09 ± 0.38%. Both male and female samples within the SS ECM group were higher than the male and female samples in the RF ECM group. The female SS ECM was higher, 5.31 ± 1.99% than the male SS ECM 4.25 ± 0.22%.

Glycosaminoglycans, more specifically CSPGs, were observed in the RF ECM following proper staining (Fig. 5, A). The total sulfated GAG content of the RF ECM was slightly higher than the total sulfated GAG content of SS ECM with 4.65 ± 0.43% and 3.94 ± 0.54% total weight (Fig. 5, B). Within the RF ECM samples the sulfated GAG content of the female samples

were similar to the sulfated GAG content of the male samples with 4.46 ± 0.16% and 4.83 ± 0.29% total weight. The female and the male SS ECM samples for the sulfated GAG content were closely related when compared to the RF ECM samples, with 3.02 ± 0.57% and 4.86 ± 0.69% total weight. Male and Female groups for all of the muscle samples were significantly different for the sulfated GAG content.

The average porosity for both RF ECM and SS ECM samples were closely related. A representation of the general porosity of each group (RF and SS ECM) is represented in (Fig. 6, A). The average porosity for the RF ECM samples as a whole was slightly higher than the SS ECM samples as a whole with 79.26 ± 5.36% and 73.65 ± 3.39% open space (Fig. 6, C). The female RF ECM samples averaged slightly lower than the male RF ECM samples, 75.25 ± 10.91% and 83.27 ± 2.02% open space. There was no significant difference with the RF ECM female and male groups even though the male samples were slightly higher. The female and male SS ECM porosity samples were more closely related than the RF samples, with 71.92 ± 5.58% and 75.38 ± 4.51% open space.

A representation of both RF ECM and SS ECM fiber alignment is represented in (Fig. 6, B). The oriented angle indicated the overall network alignment for the skeletal ECM. The RF ECM oriented angle sample has a slightly smaller angle than the SS ECM sample with 10.64 ± 1.66 degrees and 13.41 ± 2.46 degrees, respectively (Fig. 6, C). The female and male samples within the RF ECM sample group have a significant difference between them with 14.74 ± 0.71 degrees and 7.57 ± 1.43 degrees. The female and male samples within the SS ECM sample group are not significant with 11.61 ± 1.78 angle and 15.21 ± 4.78 degrees.

A representative stress/strain curve for the modulus of elasticity for both human RF ECM and SS ECM is shown in Figure 7 with the red line representing the RF ECM and the green line representing the SS ECM (Fig. 7, A). The graph shows the RF ECM for both male and female have a higher overall modulus of elasticity (kPa) than both male and female groups for the SS ECM. The overall modulus of elasticity for the RF ECM was recorded at 320 ± 109 kPa, while the overall modulus of elasticity for the SS ECM was recorded at 161 ± 43 kPa. The male RF ECM group had a slightly lower overall modulus of elasticity than the female RF ECM group with 268 ± 95 kPa and 372 ± 211 kPa, respectively. The male SS ECM group also had a lower overall modulus of elasticity than the female SS ECM with 92 ± 33 kPa and 246 ± 69 kPa (Fig. 7, B). The modulus of elasticity at 10% strain also varied within all of the ECM groups. For example, the RF ECM modulus of elasticity at 10% strain was higher than the SS ECM with 355 ± 140 kPa and 168 ± 45 kPa. The male RF ECM modulus of elasticity at 10% strain was 271 ± 98 kPa, while the female RF ECM modulus of elasticity at 10% strain was 439 ± 276 kPa. The last comparison for the modulus of elasticity at 10% strain is between the male and female SS ECM groups. The modulus of elasticity at 10% strain for the male SS ECM group was 120 ± 55 kPa and the modulus of the elasticity at 10% strain for the female SS ECM group was 227 ± 69 kPa (Fig, 7, C). Even though all the groups for both the overall modulus of elasticity and the modulus of elasticity at 10% strain were different for all the characterization parameters, no significant difference was reported.

The average diameter for the degradation of the RF ECM pellets were recorded at 3 different time points (0, 4 and 8 weeks). First, the image within Figure 8 represents the initial size of the RF ECM pellet at the time of implantation at week 0 (Fig. 8, A). Within the image, the ECM pellet is observed mid-back within the mouse. The inset within panel A is a

representation of the initial size/diameter of the RF ECM pellet in comparison to standard surgical tweezers (Fig. 8, A, inset). The initial diameter of the RF ECM pellet was recorded at 8.94 ± 0.23 mm. The 4 week diameter of the RF ECM pellet was recorded at 4.49 ± 0.44 mm, and the 8 week diameter of the RF ECM pellet was recorded at 2.10 ± 1.02 mm. The half-life for the degradation of the RF ECM pellet *in vivo* is 3.83 weeks. No statistical analysis was performed for this characterization test.

4. Discussion

A method for preparation of decellularized human RF and SS ECM samples and characterization is described in the present study. The decellularization protocol used throughout this study successfully removed cellular components, therefore ensuring the material being characterized was skeletal muscle extracellular matrix. Even though the two skeletal muscle groups were taken from two separate parts of the human body, the results for both skeletal muscle ECM types are closely related. Within certain characterization tests, the male and female groups within the same muscle ECM type showed significantly different results even though the two different muscle types did not show significant differences.

Many different techniques are used to decellularize different types of muscle. Evidence provided by our immunofluorescence staining for actin and nuclei, and by visually observing a change in color of the skeletal muscle indicated our decellularization protocol was a success. Visualization is a basic yet effective method to use when decellularizing muscle. If the initial red color of muscle is not gradually changing to a yellow/clearish color, then this is an indication of

an improper decellularization protocol. For example, an improper protocol could include: significantly low detergent concentrations used within the protocol, the decellularization technique is insufficient, or the possibility of expired detergents being used.

Visualization of gradual decellularization has been observed in different muscle types[44]. For example, a complete rat heart was confirmed to be decellularized through visual observation. Multiple detergents were compared to each other by a perfusion decellularization method. Triton-X-100 and 1% SDS were compared based on their effectiveness in removing cellular components. The rat heart that underwent Triton-X-100 decellularization was still a dull pinkish color after 12 hours of decellularization, while the rat heart decellularized with 1% SDS for the same amount of time was a white/clearish color. This color change indicates removal of cellular components.

Another method to verify decellularization is immunofluorescence staining using DAPI to identify nuclei and phalloidin to identify intercellular actin. These stains are usually performed on native muscle being used for decellularization and finished ECM. Complete decellularization within the rat heart was also verified by these staining techniques[44]. Since the decellularization method was observed through visual observations for the heart treated with 1% SDS, the SDS perfused rat heart was compared with native rat cardiac muscle. The results of the immunofluorescence staining also verified that the best detergent to completely remove cellular debris is SDS. Phalloidin and DAPI stains revealed no presence of actin or nuclei, while the native cardiac tissue was full of nuclei and actin. Our results also indicated 1% SDS along with buffer solutions and chelating agents removed cellular components. The immunofluorescence stain for nuclei and actin within native skeletal muscle and within ECM from skeletal muscle mirrored the results from the immunofluorescence stains from the whole rat heart

decellularization study. By comparing our decellularization results with other studies that used the same visual observation and immunofluorescence technique, our decellularization method was a successful protocol for decellularization of skeletal muscle.

Another method to verify decellularization of muscle is to quantify DNA by using DNA assays, more specifically the PicoGreen assay. This assay can detect DNA concentrations that are as little as 25 pg of DNA/ml of dsDNA reagent. One group has verified their decellularization method on canine quadriceps by using this particular assay[47]. This group considered their material to be decellularized when the DNA content was less than 50 ng dsDNA/mg ECM (dry weight). The DNA levels within the canine quadriceps ECM was 7.42 ng DNA/mg ECM. DNA assays, immunofluorescence staining, and visual inspection are all accepted techniques to quantify the decellularization of muscles within current literature.

When choosing a muscle type for decellularization to use as a specific treatment method, yield of ECM material and original location are important factors to consider. The yield results found within this study indicate that location and gender do not have an effect on yield of skeletal ECM. Both skeletal muscle types yielded about the same percentage of ECM. Based on the weights of each muscle type, the larger muscle would be expected to yield more ECM than the smaller muscle. Our group found that the size of the skeletal muscle is not a factor when measuring the yield of ECM from these muscles.

Different ECMs are used as treatment methods for various injuries or conditions. Some ECMs are chosen as treatment methods based on their original architecture and their original muscle location, however, some ECMs are chosen as treatment methods with no regard to the original muscle location. For example, one group chose to decellularize tibialis anterior muscle

to use as a treatment method for a volumetric muscle loss injury in the tibialis anterior region of a rat animal model[15]. The decellularized tibialis anterior muscle was chosen as the ECM used for this injury based on the original location of the skeletal muscle. Architecture of the decellularized tibialis anterior muscle is quite similar to the native architecture of the tibialis anteior muscle. This specific characteristic could promote healing within the volumetric muscle loss injury that was created. Other groups do not consider the original location of ECM when treating volumetric muscle loss sites. A different group created a volumetric muscle loss injury within a canine animal model[57]. This group used small intestinal submucosa ECM as the treatment method for the treatment of a volumetric muscle loss injury created in an Achilles tendon. The architecture and original location of the ECM did not play a role in the decision to use this material to treat the Achilles tendon injury. The results from this study did show regeneration of the Achilles tendon when the small intestinal submucosa ECM was used as the treatment method. Based on these current studies, original location and architecture is sometimes considered when choosing ECM as a treatment method.

If skeletal ECM from this study was used as a treatment method and the original location and architecture was not a factor when choosing the material then the RF ECM should be chosen. The RF ECM and the SS ECM yield the same amount of ECM, but the native RF produces a larger quantity of skeletal ECM based on the original size of the muscle. Therefore, choosing the larger muscle that weighs more would be the logical choice. If the original architecture and location needed to be considered then the quantity of ECM would not play a role in the selection of skeletal ECM.

The skeletal muscle ECM yield in this study is comparable with different ECM yields that are found within literature. For example, the decellularization of porcine pericardium ECM

and human pericardium ECM yield has been studied. The decellularization method used for that study is similar to the method used within this study. Briefly, the ionic reagent SDS and DI rinses were used to decellularize this tissue. The yield collected for porcine pericardium measured 20 mg of dry weight ECM, and the human pericardium yielded 17- 40 mg of dry weight ECM[58]. Original size of the tissue pieces before decellularize ranged between 2 to 4 cm^2. This data is presented as mg of ECM recovered, while the skeletal muscle ECM yield within this study is presented as ECM yield from percent of original weight of each piece. The porcine and human pericardium ECM and the RF ECM and SS ECM cannot be directly compared based on how the data is presented. However, being able to compare different decellularized ECM tissue type yield amounts from human or different species provides insight into how much material different types of muscle can yield.

By viewing the decellularized skeletal muscle ECM with SEM technology, our group was able to view a 3-D image of the RF ECM that identified the porosity of the skeletal ECM. The 3-D image identified individual collagen fibers along with individual pores within the skeletal muscle ECM. The human RF ECM can be compared to different types of ECM. For example, dog quadriceps of both native and decellularized ECM has been characterized[47]. For comparisons between the human RF ECM within this study and the dog skeletal muscle ECM within the Badylak study, SEM images of both the native and ECM dog skeletal muscle was observed at 500x. The 500x SEM image of native dog muscle was very structured compared to the decellularized dog skeletal muscle ECM and the human RF ECM. The native dog muscle had more alignment and more cellular components within its structure. The location of the collagen fibers within the native dog skeletal muscle were confirmed based on how the cellular components within the muscle were subdivided from each other. The SEM images of the dog

ECM and the human RF ECM were similar in that they both showed the presence of collagen fibers without cellular components attached to them. Another SEM comparison can be made with the human RF ECM and with rat heart ECM[44]. The rat heart ECM did lose some of the original architecture after the decellularization process, however the rat ECM still had evidence of collagen fibers. These same conclusions can be stated about the human RF ECM when comparing it to rat heart ECM. Comparison of the human RF ECM with two types of muscles (quadriceps and heart) from two different species (dog and rat) provides evidence that the human RF ECM has similarities to other types of ECMs.

Collagen and GAGs are a few of the main components that make up ECM. These components contribute to the different functions ECM materials are capable of performing. This makes collagen and GAG assays a desirable method in characterizing decellularized tissues/organs. By knowing which skeletal muscle ECM yields the most collagen and GAG content then the use of this skeletal ECM material could be evaluated as a specific treatment method, if needed.

The two different skeletal muscle locations have a significant effect on the collagen content of their ECM. The SS ECM collagen content doubled the RF ECM content, showing a significant difference. Since human skeletal muscle ECM has not been characterized before, there are no results to directly compare to the results found in this study. Some conclusions can be drawn from the collagen content data. Since location of the two skeletal muscles showed a significant difference, certain factors could potentially affect the collagen levels from the two different ECMs. For example, extreme exercise has been shown to make collagen levels fluctuate within the muscle that is primarily being exercised. One studied showed how the collagen levels within the quadriceps of rats that underwent high peaks of exercise for a

substantial amount of time fluctuate between high levels of collagen and normal levels of collagen[59]. Another study showed similar results as the one just mentioned, however instead of measuring the fluctuation of collagen levels in the quadriceps this study measured fluctuation of collagen levels in the supraspinatus muscle of rats[60]. Aging has been reviewed as a factor that can also affect collagen levels in skeletal muscle. A previous study showed how collagen levels within lower limb skeletal muscle experiences multiple trends in aging rats[61]. A common trend observed within this study was the dramatic increase in collagen levels within the extensor digitorum longus of rats at age (measured in days) 21 to age 86. Then the collagen levels decreased slightly from age 86 to age 188. From age 188 to age 299 collagen levels decreased dramatically compared to age 86. This suggests that age can potentially play a very important role on collagen content. By looking at some of these factors that can contribute to collagen levels and knowing that an upper skeletal ECM compared to a lower skeletal ECM has a higher collagen content, then making a decision of what type of ECM would be beneficial when using this ECM as a treatment method.

The gender did not have a significant effect on the collagen content within the two different skeletal muscle ECM groups (RF ECM and SS ECM); however the gender did have a significant effect on the GAG content within skeletal muscle ECM. GAGs play important roles within the ECM, and by knowing percent total weight of GAG in two different types of ECMs provides insight into which material would be better used as a treatment method. By knowing male and female ECM have different levels of GAGs, then using the material that contains more GAG would be more efficient when using ECM as a treatment method. More GAGs can provide the ECM with more desirable functions. For example, GAGs have been shown to interact with other ECM components to help promote intercellular signaling within the ECM[28]. GAGs have

also been shown to help with certain mechanical functions, by providing a "cushion" type response to the ECM against compression forces[28]. It is possible that the male skeletal ECM could provide more desirable functions as a treatment method since the group had a higher GAG content that the female group, but more testing would need to be conducted. Unlike quantitative measurements of collagen for specific treatments, the measurement of glycosaminoglycans are usually performed as an indication of how many GAGs are in ECM.

The collagen and GAG content from human RF ECM can be compared with other species ECMs collagen and GAG content. By comparing quadriceps ECM collagen and GAG levels from different species to the human RF ECM collagen and GAG levels, helps to verify which species quadriceps ECM yields the most collagen and GAG levels. GAG levels within native dog quadriceps and dog quadriceps ECM have been evaluated within current literature[47]. Both the native dog quadriceps and ECM were much lower than the human RF ECM GAG content found within this study with the native dog quadriceps GAG content being 3.02 ug/mg dry weight and the dog ECM being 0.61 ug/mg dry weight. This comparison shows how different species affect the GAG content of the same type of muscle ECM. The collagen levels of dog ECM was not measured within that study. Another quadriceps ECM study was performed on rats that did measure collagen content, but not GAG content[62]. The collagen content found within rat quadriceps ECM was higher than the collagen content found within the human RF ECM with the rat quadriceps ECM being 72% (assuming total weight). A possible explanation for this discovery of higher levels of collagen in rat ECM compared to human ECM could go back to the quality and the age of muscle used within this study. The rats used in the Van Dyke study were sacrificed at 4 to 7 months for characterization. Based on a study that compared rat ages to human ages, the rats sacrificed in the Van Dyke study were the equivalent of humans in their

20's[63]. This comparison of rat skeletal ECM to the human RF ECM makes sense. Having an idea of which species yields the most collagen and GAG contents definitely helps when discovering new treatment methods based on these different species skeletal muscle ECM types.

Now the human RF ECM and SS ECM can be compared to different decellularized tissue ECMs within different species. The first comparison is between rat lung ECM and the human skeletal ECM. This is a valuable comparison since some ECMs are being used as different treatment methods in multiple areas. One study characterized SDS-decellularized rat lung ECM[45]. Lung ECM is a semi-new ECM material that is being characterized within tissue engineering studies. The collagen content of rat lung ECM was higher than both the human RF ECM and SS ECM with the collagen content of rat lung ECM being 787 ug/whole lung, while the GAG content was similar for both the rat lung ECM and the human skeletal muscle ECM with the lung ECM being 20 ug/whole lung.

Different muscle types (i.e. skeletal verses smooth) can yield different amounts of cellular components when compared to each other. Porcine ECM is very well studied within tissue engineering. For example, porcine heart, dermis, bone anterior cruciate ligament (ACL), brain and spinal cord ECM have all been studied recently. Decellularized porcine heart yields more GAG levels than both human skeletal muscle ECMs with the porcine heart ECM being 125 ug GAG/mg dry ECM[58]. Collagen was shown to remain in the porcine cardiac ECM after decellularization, however the overall collagen content has yet to be studied. Another porcine ECM that has been characterized is the dermis ECM. The porcine dermis ECM yields much lower collagen and GAG amounts when compared to the human RF ECM and SS ECM with the collagen levels being 0.85 mg collagen/mg ECM and the GAG levels being 1.1 ug GAG/mg ECM[48]. When the human RF ECM and SS ECM are compared to porcine brain and spinal cord

ECMs, the GAG levels for both the brain and spinal cord ECM are lower than the human skeletal muscle ECMs[49]. The porcine brain ECM yields 5 ug GAG/mg dry weight and the spinal cord ECM yields 1.3 ug GAG/mg dry weight. However, the collagen content for the spinal cord ECM and brain ECM have much higher levels of collagen than the human skeletal muscles[49]. The brain ECM yields 538 ug collagen/mg dry weight and the spinal cord ECM yields 703 ug collagen/mg dry weight. The last comparison between the human skeletal muscle ECM and porcine is the bone ACL ECM[52]. The GAG content of the porcine ACL ECM was much lower than the human RF ECM and SS ECM with the ACL ECM being 0.07% dry weight, while the collagen content of the ACL ECM was higher than the human skeletal ECM with the ACL ECM being 86% dry weight.

The next comparison is between human pericardium ECM and human skeletal ECM. The human pericardium ECM had a higher level of GAGs when compared to both the RF ECM and SS ECM with the human pericardium ECM being 137 ug GAG/mg dry ECM[58]. The collagen content for the human pericardium ECM was not measured within that study. When looking at all of these different comparisons to human skeletal muscle ECM, one should keep in mind that every muscle type is different, especially if they are from a different species besides human. By knowing all of these comparisons between different ECMs, gives someone a rough idea of what collagen and GAG levels should be in ECM material.

The last comparison of collagen and GAG levels is between the human SS ECM and commercial ECM used in industry as a treatment method for rotator cuff repair[64]. Within that study, five commercially obtained soft tissue repair ECM materials were characterized. These commercial products are derived from multiple areas: porcine (small intestine submucosa), human (dermis), bovine (fetal dermis), and porcine (dermis). All of the commercial materials

undergo some form of removal of cellular components before they are distributed. The collagen content and the GAG content of all of the commercial ECM material used for rotator cuff repair were lower than the collagen and GAG content of the human supraspinatus ECM found within this study. Based on this comparison, human supraspinatus ECM could potentially be used as a treatment method for rotator cuff repair. A direct characterization comparison between the human SS ECM and these commercial ECM products would have to be performed before further investigation.

When engineering bioartificial scaffolds, keeping the original architecture and porosity of the desired tissue/organ is preferred. The decellularization protocol used within this study kept the original architecture and porosity intact for both the human RF ECM and SS ECM even though SDS has been known to affect these parameters in some cases[51]. The oriented angle measured within each group was an indication that skeletal muscle has an organized network alignment. The porosity values measured within this study were similar for all groups. The location and gender of skeletal muscle does not play a significant role in skeletal muscle ECM porosity measurements. The two different skeletal muscle ECM can have the same porosity measurement even though the two original skeletal muscles perform opposite functions. The oriented angle measured for the female RF ECM group and the male RF ECM group were significantly different. The female RF ECM doubled the oriented angle of the male RF ECM group indicating the female RF ECM samples are less aligned than male RF ECM samples. This could have a functional effect on the RF ECM. By knowing female RF ECM is less aligned than male RF ECM and if these ECM materials were used as a treatment method that required a more aligned piece of material, then the male skeletal RF ECM would be the best option.

If human RF ECM and SS ECM were used as a treatment method for muscle regeneration, for example, the original architecture of the muscles would be preferred if these skeletal ECM were implanted into their original locations. Currently, researchers are engineering devices to achieve some form of controllable architecture and porosity of skeletal muscle. A skeletal muscle tissue bioartificial scaffold with specific architecture and porosity has been shown to enhance cell viability in vitro[40]. Specific architecture and porosity of the engineered skeletal muscle tissue was achieved in this study by growing C2C12 rat myoblasts and primary rat skeletal myoblasts within either a fibrinogen or collagen type I hydrogel on top of a pre-determined cell aligned and porosity controlled polydimethylsiloxane (PDMS) mold. The same cell/hydrogel mixture was grown on a PDMS mold that did not have any alignment or porosity to determine if the controllable parameters affected the cell growth of the rat myoblasts. The results from this study showed that the pre-determined pore size enhanced nutrient and oxygen transfer to the myoblasts, therefore improving cell viability when compared to the mold that did not have any structural parameters[40]. Also, cell differentiation and proliferation was shown to be more effective in the pre-determined mold. The cell alignment for the pre-determined mold was slightly higher than the oriented angle found within both the human RF ECM and SS ECM. The controlled porosity was similar to the porosity of both the human RF ECM and SS ECM with the controlled porosity of the PDMS mold being about 95% porous. These specific parameters for the architecture and the porosity can help predict how cells would grow on the RF ECM and SS ECM in vivo. Further research would need to be performed on skeletal ECM in order to accurately see if a specific architecture and porosity would promote cell viability and growth in vivo.

The stiffness of the human skeletal muscle ECM was evaluated by the overall modulus of elasticity and modulus of elasticity at 10% strain. There was no significant difference for the modulus of elasticity, however the lower limb skeletal muscle ECM had a higher modulus of elasticity than the upper limb skeletal muscle ECM indicating the RF ECM is stiffer than the SS ECM. Previous studies have shown, lower limb muscles within human cadavers experience load failure at around 10% strain, therefore the modulus of elasticity at 10% strain was evaluated[65]. Upper limb skeletal muscle tendons have been studied more than the upper limb skeletal muscles themselves. Based on current literature, humans and canine supraspinatus tendons share a load failure at about 8% strain[64,66]. Keeping the same parameters (modulus of elasticity at 10% strain) for both the RF ECM and the SS ECM during mechanical testing provided consistent results based on previous strain studies.

Looking at collagen levels, GAG levels, and both modulus of elasticity's for just the combined RF ECM and SS ECM, provides insight into the skeletal ECM based on the results found. The RF ECM was higher for both modulus of elasticity's and GAG levels when compared to the SS ECM material, however the RF ECM has a lower collagen content than the SS ECM. This brings up the realization that collagen helps with mechanical loading within ECM, but GAGs also can contribute greatly to mechanical loading on ECM. Another observation can be made about the two different locations when looking at all three tests results. The collagen and collagen fibril formation was abundant within the SS ECM, however the strength of the components were weaker than the collagen present in the RF ECM. The strength of the ECM can also be traced back to the original functions of the RF and SS. The RF muscle goes through more strenuous work when compared to the SS muscle. For example, the RF muscle is used for walking, running, etc., while the SS muscle is primarily used in combination with the other four

rotator muscles to control the shoulder. By presenting all of this data about both types of skeletal muscle ECM, researchers will have a better understanding for the properties human skeletal muscle ECM. Another interesting observation from the modulus of elasticity data is that both female groups within the RF ECM and the SS ECM had a higher modulus of elasticity than both male ECM groups. This suggests that female ECM is stiffer than male ECM disregarding location of the skeletal ECM.

The modulus of elasticity at 10% strain for the SS ECM can be compared to commercial ECM used for the treatment of rotator cuff tears and canine infraspinatus tendons (part of the rotator cuff muscles), mentioned earlier in this study[64]. The method used for tensile testing of the commercial ECM products are similar to the tensile testing methods in this paper. The differences between the tensile testing methods is the load cell used for testing and the percent strain reached for the modulus of elasticity. The load cell used in this study was a 10N load cell, while the load cell used in the commercial ECM product study was either a 50 N or a 500 N load cell. In our study, we reported the modulus of elasticity at 10% strain, while the commercial ECM products were measured at 8% strain. Based on visual observations for the modulus of elasticity at 8% strain for the commercial ECM products used in treatment methods for rotator cuff repair, the product derived from human dermis has a similar modulus of elasticity at 8% strain when compared to the SS ECM modulus of elasticity at 10% strain. All of the other commercial ECM products had a slightly higher modulus of elasticity at 8% strain when compared to the SS ECM modulus of elasticity at 10% strain. Based on this observation however, the modulus of elasticity at 10% strain for the SS ECM is just as stiff as a product used in industry to treat rotator cuff injuries. Also, to note again, the collagen and GAG content for the

four commercial ECM products were all lower than the natural human skeletal ECM levels found in this study.

Degradation rate of the human skeletal ECM was evaluated within an in vivo mouse animal model. Based on the results, the diameter of the RF ECM pellet decreased in size at every time point (4 and 8 weeks). This degradation pattern was expected based on previous studies. Usually degradation studies are accompanied with repairing a defect in vivo, which was the case in a present study involving Achilles tendon regeneration in a canine animal model using decellularized small intestinal submucosa (SIS) ECM[57]. Within this study, degradation times were observed at 3 days, 1 week, 2 weeks, 3 weeks, and 8 weeks. The SIS ECM was implanted into a gap made in the Achilles tendon of female canines. By day 3 after implantation, the SIS ECM started to separate because host cells started to invade the foreign implant. This is the start of an inflammatory response. By week 1, mononuclear cells covered almost all of the ECM and new host ECM started to form. By week 2, the entire ECM implant was covered with mononuclear cells, and the original implant was 20% degraded when compared to the initial implant. By week 3, 60% of the original implant was degraded and new host ECM was observed. By week 8, the implant was completely degraded and new host ECM had taken over the defect site. The degradation time of the RF ECM in our mouse animal model also followed a decreasing trend like the one described above. By week 4 of the RF ECM degradation in the mice, 50% of the original RF ECM was degraded. Based on observations made from the previous study, inflammatory responses, more specifically, the recruitment of macrophages and neutrophils started to phagocytose the "foreign material" in the mice. By week 8 of the RF ECM degradation, 76% of the original RF ECM implant was degraded. Assuming the same inflammatory responses were still being sent to the site of implantation, the continuous decrease

in size of the RF ECM pellet was expected. Based on the degradation results and how the mice handled the implantation, human skeletal ECM could be used as a possible treatment method of some kind.

Limitations to this study were the ages of the muscle donors and the quality of muscle. This could have affected the ECM that was used for the characterization tests. Different studies have identified the average age of donors in several countries. For example, a study conducted in New Zealand, South Africa, and Ireland reported the average age of individuals who donate their body to science are between 60-69 years old[67]. These findings correlate with the average age of donors used within this study, with the average age of muscle used being 71 years old.

Since the donors were older, the quality of their skeletal muscle could have affected the characteristics of the ECM. For example, muscle fibers within young and older individuals have been characterized and compared to each other in current literature. Muscle fibers, specifically type I (slow-twitch) and type II (fast-twitch), found within skeletal muscle significantly decreases in size within individuals in their 50's[68]. Muscle fiber size start to slowly decrease in number after an individual turns 25 years old, but when individuals become middle aged muscle fibers decrease in size faster than before. The size of skeletal muscle fibers indicate the overall skeletal muscle mass. This evidence indicates younger individuals have more muscle mass than individuals who are 50 years old and above. ECM surrounding these muscles start to shrink when muscle mass decreases in older individuals, causing less available ECM from older donors when compared to younger donors.

Within a different study, quadriceps strength and cross sectional area have been characterized in both young and old men and young and old women[69,70]. Within the female

groups, young individuals were 20-29 years old and older individuals were 71-81 years old. Within the male groups, young individuals were 21 to 28 years old and the older individuals were 70-79 years old. Within the young and old female groups, young individuals weighed 50 to 73 kg, while the old weighed 43 to 88 kg. Within the young and old male groups, young individuals weighed 65 to 82 kg while the old individuals weighed 66 to 83 kg.

Muscle strength in the old female group was shown to be 35% weaker than the young female group, and the cross sectional area of the quadriceps in the old female group was 33% less than the young female group. The difference in weight of the young and old females indicate that the old group was slightly heavier than the young group. This weight difference could have affected the quadriceps strength within the old group. This indicates both age and weight can play a role in muscle mass and strength, which affects the ECM.

The muscle strength in the old male group was 39% weaker than the young male group. The old male group had 25% less muscle mass than the young male group even though the body weights of both male groups were practically the same. The male and female groups within these studies were not compared with each other. The data collected from the two male groups indicate that even if two sets of different groups have the same body weight, this does not guarantee that the identical muscles within each group weigh the same. This can be from muscle degeneration from old age or more percent body fat than muscle mass. Based on the data provided from these two studies and the weights and ages recorded within this study, donors can vary greatly in muscle function or muscle size when compared to each regardless of gender. By comparing skeletal muscle mass within male and female groups, more specifically young and old, male and female, provides insight into the ECM that is essentially yielded from these different types of skeletal muscles.

5. Conclusions

The key findings of this study suggest:

- Our group is the first to characterize human skeletal muscle extracellular matrix.
- Location and gender do not have a significant effect on the yield, mechanics, and porosity characteristics of human skeletal muscle extracellular matrix.
- Gender within the rectus femoris skeletal muscle extracellular matrix does have a significant effect on the network alignment. The overall location and gender does not have a significant effect on the network alignment of human skeletal muscle extracellular matrix.
- Location (upper limb muscle vs. lower limb muscle) and gender does have a significant effect on the chemical characteristics of human skeletal muscle extracellular matrix.
- The human skeletal muscle extracellular matrix can be tolerated within an in-vivo animal model without complications.

6. References

1. Jarvinen TA, Jarvinen TL, Kaariainen M, Kalimo H, Jarvinen M. Muscle injuries: Biology and treatment. *Am J Sports Med*. 2005;33(5):745-764.

2. Gillies AR, Lieber RL. Structure and function of the skeletal muscle extracellular matrix. *Muscle Nerve*. 2011;44(3):318-331.

3. Mair SD, Seaber AV, Glisson RR, Garrett WE,Jr. The role of fatigue in susceptibility to acute muscle strain injury. *Am J Sports Med*. 1996;24(2):137-143.

4. Chan YS, Li Y, Foster W, et al. Antifibrotic effects of suramin in injured skeletal muscle after laceration. *J Appl Physiol (1985)*. 2003;95(2):771-780.

5. Almekinders LC. Anti-inflammatory treatment of muscular injuries in sport. *Sports Medicine*. 1999;28(6):383-388.

6. Cantini M, Carraro U. Macrophage-released factor stimulates selectively myogenic cells in primary muscle culture. *Journal of Neuropathology & Experimental Neurology*. 1995;54(1):121-128.

7. MAURO A. Satellite cell of skeletal muscle fibers. *J Biophys Biochem Cytol*. 1961;9:493-495.

8. Cornelison D, Wold BJ. Single-cell analysis of regulatory gene expression in quiescent and activated mouse skeletal muscle satellite cells. *Dev Biol*. 1997;191(2):270-283.

9. Tatsumi R, Liu X, Pulido A, et al. Satellite cell activation in stretched skeletal muscle and the role of nitric oxide and hepatocyte growth factor. *Am J Physiol Cell Physiol*. 2006;290(6):C1487-94.

10. Conboy IM, Rando TA. The regulation of notch signaling controls satellite cell activation and cell fate determination in postnatal myogenesis. *Developmental cell*. 2002;3(3):397-409.

11. Brack AS, Conboy IM, Conboy MJ, Shen J, Rando TA. A temporal switch from notch to wnt signaling in muscle stem cells is necessary for normal adult myogenesis. *Cell stem cell*. 2008;2(1):50-59.

12. Gentile NE, Stearns KM, Brown EH, et al. Targeted rehabilitation after extracellular matrix scaffold transplantation for the treatment of volumetric muscle loss. *Am J Phys Med Rehabil*. 2014;93(11 Suppl 3):S79-87.

13. Owens BD, Kragh JF,Jr, Wenke JC, Macaitis J, Wade CE, Holcomb JB. Combat wounds in operation iraqi freedom and operation enduring freedom. *J Trauma*. 2008;64(2):295-299.

14. Lin CH, Lin YT, Yeh JT, Chen CT. Free functioning muscle transfer for lower extremity posttraumatic composite structure and functional defect. *Plast Reconstr Surg*. 2007;119(7):2118-2126.

15. Corona BT, Wu X, Ward CL, McDaniel JS, Rathbone CR, Walters TJ. The promotion of a functional fibrosis in skeletal muscle with volumetric muscle loss injury following the transplantation of muscle-ECM. *Biomaterials*. 2013;34(13):3324-3335.

16. Mase VJ,Jr, Hsu JR, Wolf SE, et al. Clinical application of an acellular biologic scaffold for surgical repair of a large, traumatic quadriceps femoris muscle defect. *Orthopedics*. 2010;33(7):511-20100526-24.

17. Sicari BM, Agrawal V, Siu BF, et al. A murine model of volumetric muscle loss and a regenerative medicine approach for tissue replacement. *Tissue Engineering Part A*. 2012;18(19-20):1941-1948.

18. Sicari BM, Rubin JP, Dearth CL, et al. An acellular biologic scaffold promotes skeletal muscle formation in mice and humans with volumetric muscle loss. *Sci Transl Med*. 2014;6(234):234ra58.

19. Hurd SA, Bhatti NM, Walker AM, Kasukonis BM, Wolchok JC. Development of a biological scaffold engineered using the extracellular matrix secreted by skeletal muscle cells. *Biomaterials*. 2015;49(0):9-17.

20. Duance V, Restall D, Beard H, Bourne F, Bailey A. The location of three collagen types in skeletal muscle. *FEBS Lett*. 1977;79(2):248-252.

21. Eggen KH, Malmstrøm A, Kolset SO. Decorin and a large dermatan sulfate proteoglycan in bovine striated muscle. *Biochimica et Biophysica Acta (BBA)-Protein Structure and Molecular Enzymology*. 1994;1204(2):287-297.

22. DeQuach JA, Mezzano V, Miglani A, et al. Simple and high yielding method for preparing tissue specific extracellular matrix coatings for cell culture. *PloS one*. 2010;5(9):e13039.

23. Gilbert TW, Wognum S, Joyce EM, Freytes DO, Sacks MS, Badylak SF. Collagen fiber alignment and biaxial mechanical behavior of porcine urinary bladder derived extracellular matrix. *Biomaterials*. 2008;29(36):4775-4782.

24. Kesava Reddy G, Enwemeka CS. A simplified method for the analysis of hydroxyproline in biological tissues. *Clin Biochem*. 1996;29(3):225-229.

25. van der Rest M, Garrone R. Collagen family of proteins. *FASEB J*. 1991;5(13):2814-2823.

26. Chastain SR, Kundu AK, Dhar S, Calvert JW, Putnam AJ. Adhesion of mesenchymal stem cells to polymer scaffolds occurs via distinct ECM ligands and controls their osteogenic differentiation. *Journal of Biomedical Materials Research Part A*. 2006;78(1):73-85.

27. Bosnakovski D, Mizuno M, Kim G, Takagi S, Okumura M, Fujinaga T. Chondrogenic differentiation of bovine bone marrow mesenchymal stem cells (MSCs) in different hydrogels: Influence of collagen type II extracellular matrix on MSC chondrogenesis. *Biotechnol Bioeng*. 2006;93(6):1152-1163.

28. Hardingham TE, Fosang AJ. Proteoglycans: Many forms and many functions. *FASEB J*. 1992;6(3):861-870.

29. Brandan E, Inestrosa NC. Isolation of the heparan sulfate proteoglycans from the extracellular matrix of rat skeletal muscle. *J Neurobiol*. 1987;18(3):271-282.

30. Velleman SG, Patterson RA, Nestor KE. Identification of decorin and chondroitin sulfate proteoglycans in turkey skeletal muscle. *Poult Sci*. 1997;76(3):506-510.

31. Bidanset DJ, Guidry C, Rosenberg LC, Choi HU, Timpl R, Hook M. Binding of the proteoglycan decorin to collagen type VI. *J Biol Chem*. 1992;267(8):5250-5256.

32. Schmidt G, Robenek H, Harrach B, et al. Interaction of small dermatan sulfate proteoglycan from fibroblasts with fibronectin. *J Cell Biol*. 1987;104(6):1683-1691.

33. Yamada KM, Kennedy DW, Kimata K, Pratt RM. Characterization of fibronectin interactions with glycosaminoglycans and identification of active proteolytic fragments. *J Biol Chem*. 1980;255(13):6055-6063.

34. Carrino DA, Oron U, Pechak DG, Caplan AI. Reinitiation of chondroitin sulphate proteoglycan synthesis in regenerating skeletal muscle. *Development*. 1988;103(4):641-656.

35. Sugrue SP, Hay ED. Response of basal epithelial cell surface and cytoskeleton to solubilized extracellular matrix molecules. *J Cell Biol*. 1981;91(1):45-54.

36. Murray JC, Stingl G, Kleinman HK, Martin GR, Katz SI. Epidermal cells adhere preferentially to type IV (basement membrane) collagen. *J Cell Biol*. 1979;80(1):197-202.

37. Terranova VP, Rohrbach DH, Martin GR. Role of laminin in the attachment of PAM 212 (epithelial) cells to basement membrane collagen. *Cell*. 1980;22(3):719-726.

38. Williams CM, Engler AJ, Slone RD, Galante LL, Schwarzbauer JE. Fibronectin expression modulates mammary epithelial cell proliferation during acinar differentiation. *Cancer Res*. 2008;68(9):3185-3192.

39. Badylak SF, Freytes DO, Gilbert TW. Extracellular matrix as a biological scaffold material: Structure and function. *Acta biomaterialia*. 2009;5(1):1-13.

40. Bian W, Bursac N. Engineered skeletal muscle tissue networks with controllable architecture. *Biomaterials*. 2009;30(7):1401-1412.

41. Seif-Naraghi SB, Singelyn JM, Salvatore MA, et al. Safety and efficacy of an injectable extracellular matrix hydrogel for treating myocardial infarction. *Sci Transl Med*. 2013;5(173):173ra25.

42. Montoya CV, McFetridge PS. Preparation of ex vivo–based biomaterials using convective flow decellularization. *Tissue Engineering Part C: Methods*. 2009;15(2):191-200.

43. Baptista PM, Orlando G, Mirmalek-Sani S, Siddiqui M, Atala A, Soker S. Whole organ decellularization-a tool for bioscaffold fabrication and organ bioengineering. . 2009:6526-6529.

44. Ott HC, Matthiesen TS, Goh S, et al. Perfusion-decellularized matrix: Using nature's platform to engineer a bioartificial heart. *Nat Med*. 2008;14(2):213-221.

45. Petersen TH, Calle EA, Colehour MB, Niklason LE. Matrix composition and mechanics of decellularized lung scaffolds. *Cells Tissues Organs*. 2012;195(3):222-231.

46. Young DA, Ibrahim DO, Hu D, Christman KL. Injectable hydrogel scaffold from decellularized human lipoaspirate. *Acta Biomaterials*. 2011;7(3):1040-1049.

47. Wolf MT, Daly KA, Reing JE, Badylak SF. Biologic scaffold composed of skeletal muscle extracellular matrix. *Biomaterials*. 2012;33(10):2916-2925.

48. Wolf MT, Daly KA, Brennan-Pierce EP, et al. A hydrogel derived from decellularized dermal extracellular matrix. *Biomaterials*. 2012;33(29):7028-7038.

49. Medberry CJ, Crapo PM, Siu BF, et al. Hydrogels derived from central nervous system extracellular matrix. *Biomaterials*. 2013;34(4):1033-1040.

50. Singelyn JM, Sundaramurthy P, Johnson TD, et al. Catheter-deliverable hydrogel derived from decellularized ventricular extracellular matrix increases endogenous cardiomyocytes and preserves cardiac function post-myocardial infarction. *Journal of the American College of Cardiology*. 2012;59(751-763).

51. Gilbert TW, Sellaro TL, Badylak SF. Decellularization of tissues and organs. *Biomaterials*. 2006;27(19):3675-3683.

52. Woods T, Gratzer PF. Effectiveness of three extraction techniques in the development of a decellularized bone–anterior cruciate ligament–bone graft. *Biomaterials*. 2005;26(35):7339-7349.

53. Chiriboga L, Yee H, Diem M. Infrared spectroscopy of human cells and tissue. part VII: FT-IR microspectroscopy of DNase-and RNase-treated normal, cirrhotic, and neoplastic liver tissue. *Appl Spectrosc*. 2000;54(4):480-485.

54. Liu B, Qu M, Qin K, et al. Role of cyclic strain frequency in regulating the alignment of vascular smooth muscle cells in vitro. *Biophys J*. 2008;94(4):1497-1507.

55. Huang NF, Lee RJ, Li S. Engineering of aligned skeletal muscle by micropatterning. *Am J Transl Res*. 2010;2(1):43-55.

56. Edwards C, O'brien W. Modified assay for determination of hydroxyproline in a tissue hydrolyzate. *Clinica chimica acta*. 1980;104(2):161-167.

57. Gilbert TW, Stewart-Akers AM, Simmons-Byrd A, Badylak SF. Degradation and remodeling of small intestinal submucosa in canine achilles tendon repair. *The Journal of Bone & Joint Surgery*. 2007;89(3):621-630.

58. Seif-Naraghi SB, Salvatore MA, Schup-Magoffin PJ, Hu DP, Christman KL. Design and characterization of an injectable pericardial matrix gel: A potentially autologous scaffold for cardiac tissue engineering. *Tissue Engineering Part A*. 2010;16(6):2017-2027.

59. Langberg H, Skovgaard D, Asp S, Kjaer M. Time pattern of exercise-induced changes in type I collagen turnover after prolonged endurance exercise in humans. *Calcif Tissue Int*. 2000;67(1):41-44.

60. Soslowsky L, Thomopoulos S, Tun S, et al. Neer award 1999: Overuse activity injures the supraspinatus tendon in an animal model: A histologic and biomechanical study. *Journal of Shoulder and Elbow Surgery*. 2000;9(2):79-84.

61. Alnaqeeb MA, Al Zaid NS, Goldspink G. Connective tissue changes and physical properties of developing and ageing skeletal muscle. *J Anat*. 1984;139 (Pt 4)(Pt 4):677-689.

62. Stern MM, Myers RL, Hammam N, et al. The influence of extracellular matrix derived from skeletal muscle tissue on the proliferation and differentiation of myogenic progenitor cells ex vivo. *Biomaterials*. 2009;30(12):2393-2399.

63. Sengupta P. The laboratory rat: Relating its age with human's. *International journal of preventive medicine*. 2013;4(6):624.

64. Derwin KA, Baker AR, Spragg RK, Leigh DR, Iannotti JP. Commercial extracellular matrix scaffolds for rotator cuff tendon repair. biomechanical, biochemical, and cellular properties. *J Bone Joint Surg Am*. 2006;88(12):2665-2672.

65. Van Ee C, Chasse A, Myers B. Quantifying skeletal muscle properties in cadaveric test specimens: Effects of mechanical loading, postmortem time, and freezer storage. *J Biomech Eng*. 2000;122(1):9-14.

66. Huang C, Wang VM, Pawluk RJ, et al. Inhomogeneous mechanical behavior of the human supraspinatus tendon under uniaxial loading. *Journal of orthopaedic research*. 2005;23(4):924-930.

67. Cornwall J, Perry GF, Louw G, Stringer MD. Who donates their body to science? an international, multicenter, prospective study. *Anatomical sciences education*. 2012;5(4):208-216.

68. Lexell J. Human aging, muscle mass, and fiber type composition. *J Gerontol A Biol Sci Med Sci*. 1995;50 Spec No:11-16.

69. Young A, Stokes M, Crowe M. Size and strength of the quadriceps muscles of old and young women*. *Eur J Clin Invest*. 1984;14(4):282-287.

70. Young A, Stokes M, Crowe M. The size and strength of the quadriceps muscles of old and young men. *Clin Physiol*. 1985;5(2):145-154.

7. Appendix

Figure 1

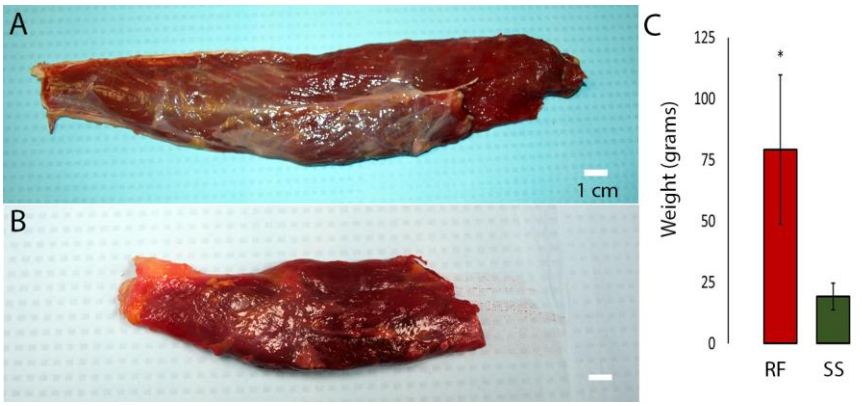

Fig. 1. Representative image of whole human RF (A) and SS (B). Average weights of whole RF and SS used for characterization tests in grams (C). Data is presented as mean ± standard deviation. Significant difference (P = 0.001) was recorded between whole RF and SS weight groups using a student t-test with equal variance indicated with an asterisk. Photo by author.

Table 1

Table 1
Comparison of tissue age in Rectus Femoris and Supraspinatus

	Average Age	Female	Male	Age Range
Rectus Femoris	70.0 ± 22.1	65.4 ± 22.2	74.6 ± 22.5	24 - 98
Supraspinatus	65.8 ± 22.9	65.4 ± 20.1	66.2 ± 27.8	24 - 95

Table 1. Average age of all muscles used for characterization tests. Data is presented as mean ± standard deviation. Number of skeletal muscles used for characterization tests were RF, n = 16 and SS, n = 10.

Figure 2

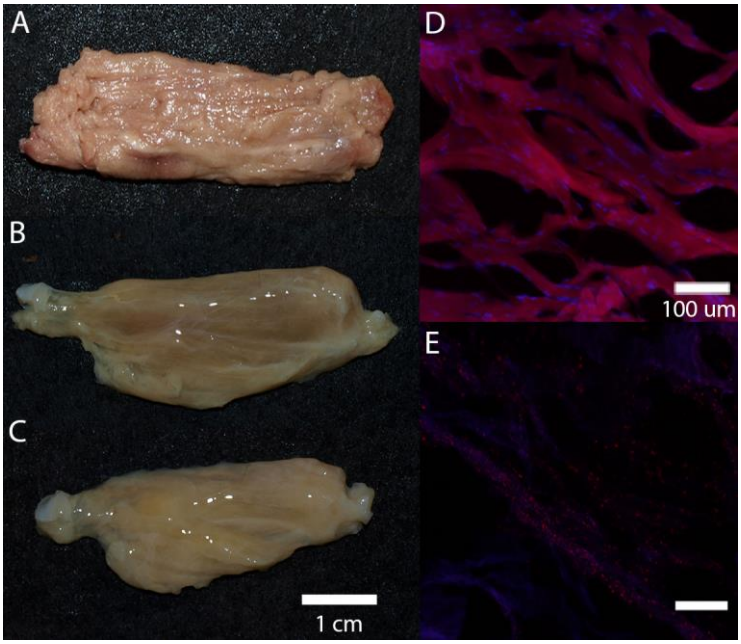

Fig. 2. Progressive decellularization RF samples at Day 0, 5, and 15 (A-C). Fluorescently stained nuclei (DAPI-Blue) and intercellular actin (Phalloidin-Red) in non-decellularized (D) native RF muscle and decellularized RF ECM (E) at 200x. Photos by author.

Figure 3

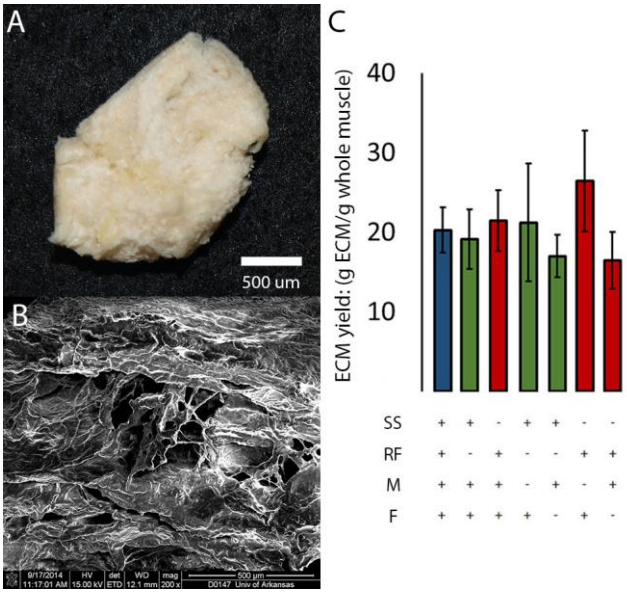

Fig. 3. Representation of yield RF ECM from decellularization protocol (A). SEM representation image of RF ECM at 200x (B). Average ECM yield (g ECM/g whole muscle) for all groups (C). Data presented as mean ± the standard error of the mean. No significant difference reported. Photo by author.

Figure 4

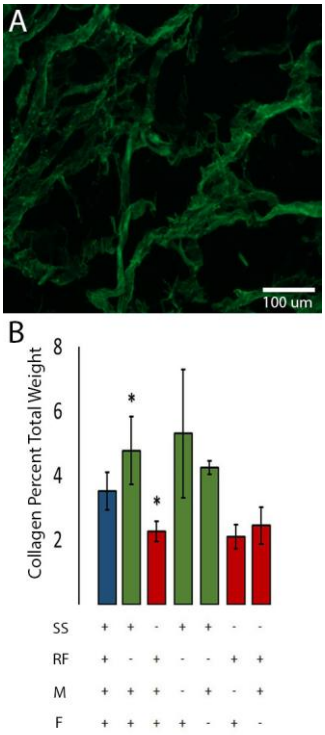

Fig. 4. Representative of collagen (green) in RF ECM (A). Average collagen composition for all groups (B). Data presented as mean ± the standard error of the mean. Significant difference between location was recorded ($P<0.05$) between the RF ECM and SS ECM using a 2-way ANOVA indicated with an asterisk.

Figure 5

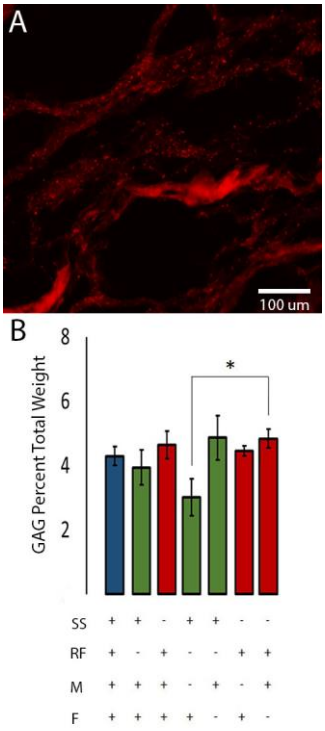

Fig. 5. Representative of chondroitin sulfate proteoglycan (GAG-red) in RF ECM (A). Average GAG composition for all groups (B). Data presented as mean ± the standard error of the mean. Significant difference for the overall gender regardless of location was recorded ($P<0.05$) for the skeletal ECM using a 2-way ANOVA indicated with an asterisk.

Figure 6

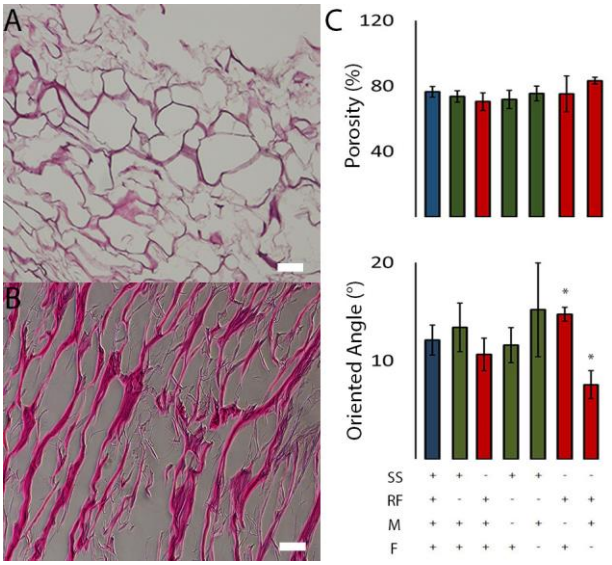

Fig. 6. Representative of porosity (A) and oriented angle (B) in RF ECM (100x). Scale bars are 100 um. Average porosity (% open space) (C) and oriented angle (degrees) (D) for all groups. Data presented as mean ± the standard error of the mean. Significant difference ($P<0.05$) was recorded between gender of the RF ECM group using a student t-test with equal variance indicated with an asterisk.

Figure 7

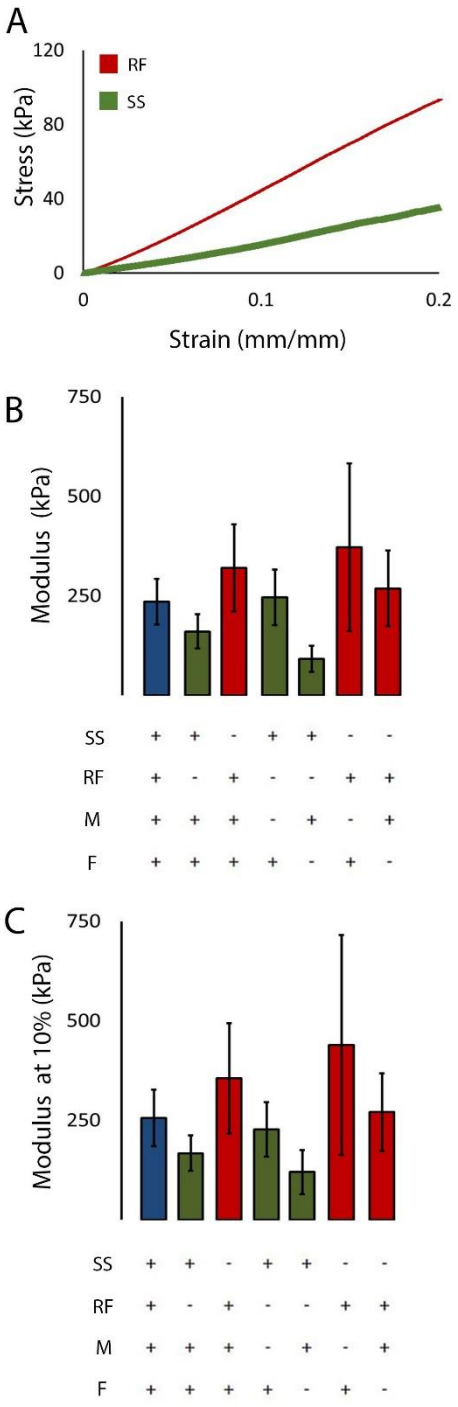

Fig. 7. Stress (kPa) / Strain (mm/mm) curves for overall modulus of elasticity with red representing RF ECM and green representing SS ECM (A). Overall Modulus of Elasticity (kPa) (B) and Modulus of Elasticity (kPa) at 10% strain (C) were identified from the corresponding stress/strain curves. No significant difference was reported. Data presented as mean ± the standard error of the mean.

Figure 8

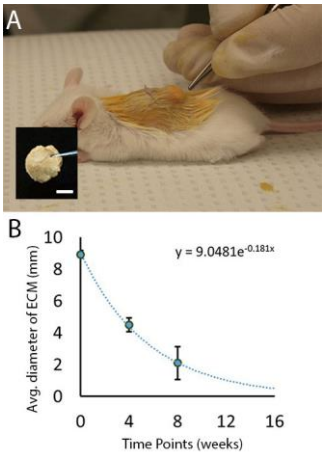

Fig. 8. Representative of mice after initial implantation of RF ECM pellet (A) with an inset representing the size of the ECM pellet. The scale bar within the inset is 5 mm. Degradation curve with the average diameter of the ECM (mm) at 3 time points (0, 4, and 8 weeks) (B). The half-life of the ECM pellet is 3.83 weeks. Data presented as mean ± the standard error of the mean. Photo by author.